Network Development During Epoxy Curing: Experimental Ultrasonic Data and Theoretical Predictions

*C. Pindinelli, G. Montagna[§], V.A.M. Luprano[§] and A. Maffezzoli**

Department of Innovation Engineering, University of Lecce
Via Monteroni 73100, Lecce, Italy; Email: alfonso.maffezzoli@unile.it
[§]PASTIS-CNRSM, Brindisi Italy

Summary: Ultrasonic waves propagation acts as a dynamic mechanical deformation on a material. When, during ultrasonic wave propagation, chemical or physical changes occurs, the evolution of an elastic modulus can be monitored. Therefore, this technique can be considered a powerful tool for non-destructive cure monitoring with a potential for "in situ" applications. In this work, the isothermal cure of a model epoxy resin cured with an amine is studied using propagation of longitudinal ultrasonic wave. The epoxy to amine ratio is optimized in order to reach full conversion of the amine groups during curing. The relative changes in the ultrasonic velocity and attenuation, measured by the transmission technique, have been applied to the calculation of the longitudinal modulus. The ultrasonic modulus has been compared with the degree of reaction measured using Differential Scanning Calorimetry (DSC). Furthermore a correlation between the ultrasonic modulus and the crosslinking density is presented combining DSC data with the stoichiometry of reactants according with the statistical theory of Miller and Macosko. The plot of the ultrasonic modulus as a function of the crosslinking density suggested that the theory of rubber elasticity can not be applied to the ultrasonic bulk longitudinal modulus as a consequence of the small deformation involved in the propagation of the ultrasonic waves.

Introduction

Ultrasonic inspection for non destructive analysis is routinely applied to the quality control presenting among other advantages the reliability and the cost. However, when chemical or physical changes in a material are associated with significant changes of the elastic constants, it is possible to characterize the evolution of their mechanical properties by means of acoustic measurements. Ultrasonic waves act as a high frequency dynamic-mechanical deformation applied to the material, leading to the determination of the loss and storage moduli and of the loss factor of the material. Only recently the potential application of acoustic wave propagation in the cure monitoring

© WILEY-VCH Verlag GmbH, 69469 Weinheim, 2002 CCC 1022-1360/00/$ 17.50+.50/0

of thermosetting resins has been presented[1-4]. However, the correlation of the ultrasonic moduli changes with the development of the crosslinked structure has not been yet analyzed.

In this work, the isothermal crosslinking of a model epoxy resin cured with an exa-functional amine is studied using propagation of longitudinal ultrasonic wave. The epoxy to amine ratio is optimized in order to reach full conversion of the amine groups during curing. The relative changes in the ultrasonic velocity and attenuation, measured by the transmission technique, have been applied to the calculation of the longitudinal modulus. The ultrasonic modulus has been compared with the degree of reaction measured using a Differential Scanning Calorimeter (DSC). Furthermore a correlation between the ultrasonic modulus and the crosslinking density is presented combining DSC data with the stoichiometry of reactants according with the statistical theory of Miller and Macosko[5, 6].

Experimental

The studied resin system was a mixture of a DGEBA (diglycidyl ether of bisphenol A) based epoxy resin (Epon 828 from Shell) characterized by an epoxy equivalent weight (EEW) of 188 g/mol and an aliphatic exa-amine curing agent (Three Ethylene Tetra Amine) from Aldrich. The choice of an amine to epoxy ratio equal to 7.2 Phr (part of amine for a hundred part of resin by weight) is described below.

The cure is analysed using a differential scanning calorimeter (DSC) Perkin-Elmer DSC-7 operating in isothermal and non-isothermal conditions in presence of a nitrogen flux of 20 ml/min.

The longitudinal velocity and the ultrasonic wave attenuation during the cure at different temperatures are measured modifying the parallel plate rheometer Rheometric ARES. ARES oven and gap control system are used during ultrasonic measurements. Two custom made ultrasonic transducers, operating up to 100 °C, are fitted into the parallel plate disposable tools of the rheometer. The transducers are connected to a pulser-receiver system Panametrics 9100 providing a digital output and measurements are performed in the transmission mode filtering frequencies in the range of 2-4 MHz. The gap between the two transducers is measured using the ARES data acquisition software while ultrasonic data are processed in a separate computer and longitudinal velocity and attenuation are recorded every 9 s. A sketch of the apparatus is reported in Fig.1. The ultrasonic measurements were performed in isothermal conditions by placing

the resin sample, in form of a thin sheet (less than 1 mm), into the preheated oven in contact with the transducers. Aluminum foils and a coupling gel are used for preserving transducer integrity and at the same time to optimize the ultrasonic coupling. The contraction of the resin during cure is measured and followed by the vertical movement of the upper transducer, driven by the gap control function of the rheometer. Isothermal ultrasonic and DSC measurements were obtained at the same temperatures.

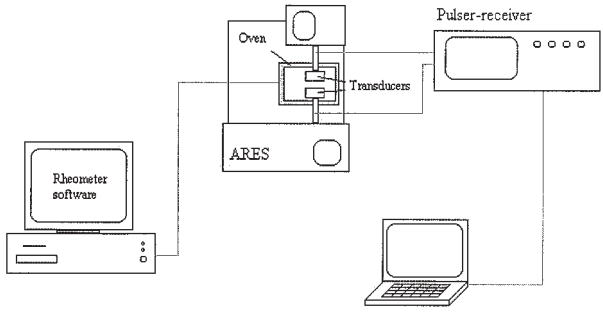

Figure 1. Sketch of the experimental apparatus for ultrasonic cure monitoring.

DSC analysis

Diffusion effects during cure

The degree of reaction (α_{DSC}) is calculated in isothermal DSC experiments following a classical procedure previously reported[4]. As shown in Table 1, the heat developed during isothermal DSC experiments (Q_{is}) is lower than maximum heat of reaction measured in non-isothermal scans Q_{tot}=428 J/g indicating that unreacted groups are still present.

Table 1. Heat of reaction, maximum degree of reaction and for isothermal curing of 7.2 Phr composition sample at various cure temperatures.

Cure Temperature	50°C	55°C	60°C	65°C	70°C
Q_{is} (J/g)	368.08	389.48	402.32	415.16	423.72
α_{max}	0.86	0.91	0.94	0.97	0.99
T_g	62°C	69°C	73°C	80°C	86°C

Curing rate of epoxy-amine reaction may be controlled either by chemical reactivity of functional groups either by diffusion of reacting species. During curing the reaction is initially controlled by chemical reactivity of amine and epoxy groups and the rate of reaction is independent of the diffusion constants of the species carrying these functional groups. As high crosslinking densities are reached, the diffusion of reactants significantly affects the reaction kinetics. In the last stage of the cure, epoxy-amine reaction is no long associated with small molecules migration, but it involves displacements of long branched molecules and segmental mobility of network. Therefore, steric hindrances and slow segmental diffusion lower the curing rate and lead to a reaction diffusion-controlled. Furthermore, segmental mobility is dramatically decreased by vitrification. In fact, the glass transition temperature of the growing network, continuously increasing during cure, approaches the isothermal cure temperature strongly reducing the molecular mobility. In these conditions, the reaction is slower and the cure, in practice, is arrested.

Isothermal data for degree of reaction (α_{DSC}) are obtained for curing of 7.2 Phr composition samples, lead at temperatures of 50°C, 55°C, 60°C, 65°C and 70°C. These data are analysed in order to show the dependence of curing reaction on diffusion as vitrification of resin is approached. As long as curing is controlled by chemical reactivity of reacting functional groups, the degree of reaction is described by the following differential equation:

$$\frac{d\alpha}{dt} = k(T)f(\alpha) \tag{1}$$

where $f(\alpha)$ is a function of the degree of reaction and $k(T)$ is the reaction rate constant. The dependence of k on absolute temperature T is governed by Arrhenius expression:

$$k = A\exp\left(-\frac{E_a}{RT}\right) \tag{2}$$

where E_a is the activation energy and R is the gas constant (R=8.314 J/molK).

Assuming that the reaction is controlled by chemical reactivity, Eq.1 is valid at any temperature. A change of the experimental temperature affects the value of the rate constant, while the degree of reaction still follows Eq.1. Therefore, it is possible to superimpose the curves of degree of reaction as a function of time, obtained at different cure temperatures simply modifying the experimental time scale[7]. This time-temperature superposition is obtained using a shift factor, a_T, for the time scale

assuming as reference temperature 70°C (a_T=1 for T=70°C). Table 2 shows the values of a_T for the different temperatures considered. The time dependence of the degree of reaction obtained in isothermal experiments at different temperatures is shown in Fig.2a while the superposition of curves resulting from the use of the ~~by-the-~~shift factor a_T is reported in Fig.2b.

Table 2. Shift factor, maximum degree of reaction and degree of reaction at the transition to diffusion control at different cure temperatures.

Cure temperature	a_T	α_{max}	α_{lim}
50°C	0,26	0,86	0,75
55°C	0,38	0,91	0,79
60°C	0,50	0,94	0,82
65°C	0,72	0,97	0,85
70°C	1	0,99	-

As shown in Fig.2b, isothermal curves superimpose in the first stage of the process, when reaction is controlled by chemical reactivity; for higher values of α_{DSC} the reaction is slowered by the growth of the network and the reduction of segmental mobility due to vitrification. For high degrees of conversion the reaction becomes diffusion-controlled and superimposition is no long observed. This effect is stronger at lower reaction temperature, because diffusion is more difficult and the resin approaches vitrification temperature earlier as cure temperature is lower. As a consequence, the maximum value of the degree of reaction reached is higher for curing lead at higher cure temperature.

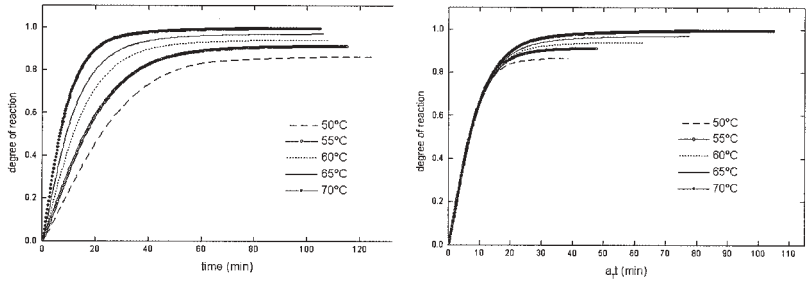

Figure 2. Plot of degree of reaction vs time: a) raw DSC data; b) superimposition of curves by shift factor a_T.

Table 2 reports the value of α at which reaction becomes diffusion controlled (α_{lim}) for each temperature considered. As shown in Table 2, although α_{lim} and α_{DSC} have been calculated following different procedures, they are characterized by the same increment with the cure temperature. This may be explained taking into account that the values of both α_{lim} and α_{DSC} result from the effect of diffusion on the reaction. Fig.3 shows the region of Fig.2b where the transition to the diffusion control mechanism occurs. Referring to the first stage of the reaction, when chemical reactivity control occurs, from eq.1 it can be obtained[7]:

$$\frac{k(T)}{a_T(T)} = \frac{\frac{d\alpha}{dt}}{f(\alpha)} = C_1 \tag{3}$$

where C_1 is a constant. Thus, at any temperature, the ratio of the rate constant and the shift factor is a constant and it does not depend on the temperature. Substituting Arrhenius equation for k(T), the following expression for a_T is obtained:

$$a_T(T) = \frac{1}{C_1}\exp\left(-\frac{E_a}{RT}\right) \tag{4}$$

Experimental data of shift factor obtained from isothermal measurements fit very well with Eq.4 and their analysis gives $C_1=1.295*10^{-8}$ and $E_a=12.413$ kcal/mol.

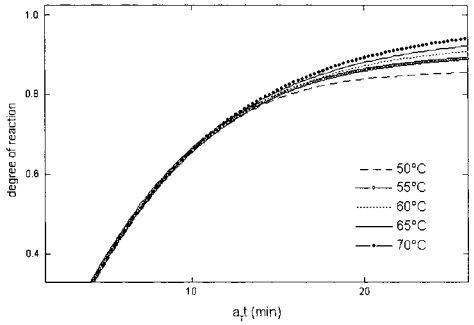

Figure 3. Transition from chemical reactivity control to diffusion control.

Therefore the development of a high density network may lead to incomplete reaction of amine or epoxy group as a consequence of the so called caging effect[8]. This effect is highlighted in Fig.4, where the heat of reaction for unit mass of amine during dynamic scans (Q_A) is reported as a function weight fraction of amine. As shown in this figure,

for amine content lower than 8 Phr, a plateau is approached indicating full conversion of amine groups.

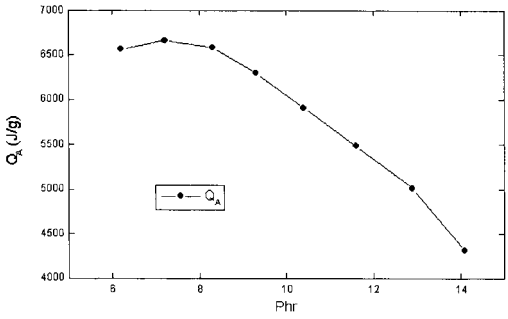

Figure 4. Heat of reaction for unit mass of amine (Q_A) as a function weight fraction of amine in Parts per hundred parts of resin (Phr).

Choice of amine/epoxy ratio

The theoretical stoichiometric ratio of amine to epoxy is 12.9 Phr. This results is confirmed by DSC analysis as the value corresponding to the maximum heat of reaction in a dynamic scan at 10°C/min. However, in view of a correlation of postgel network properties with ultrasonic data, the resin formulation must be properly chosen accounting for:

1. the maximum temperature for ultrasonic measurements (100 °C)
2. the value of the degree of reaction at the gel point (α_{gel}) depending on the functionality of amine (f_A) and epoxy (f_E) and from the stoichiometric ratio r[9]:

$$\alpha_{gel} = \frac{1}{\sqrt{r(f_A - 1)(f_E - 1)}} \tag{5}$$

3. the maximum value of the glass transition temperature (T_g) of the resin. T_g must be kept under 100 °C in order to perform at least an ultrasonic experiment leading to a final degree of reaction equal to 1.
4. Finally, as shown formerly in Fig.4, a full conversion of amine groups may be reached only for a large excess of epoxy.

On the basis of these considerations a formulation containing 7.2 Phr is chosen. For this formulation the T_g = 91 °C and α_{gel}=0.6 from Eq.5 and α_{DSC} may be assumed equal to the conversion of amine groups (p_A). This assumption represents a key point for the calculation of the crosslinking density through the statistical approach reported below.

Ultrasonic analysis

Velocity at five different temperatures are reported in Fig.5. The initial values decrease with temperature as expected[4] while the final values increase with the cure temperature. Since at higher temperatures are associated higher maximum values of the degree of reaction and hence higher crosslinking density, this result indicates that for the studied resin is more significant the effect of crosslinking compared with that of temperature.

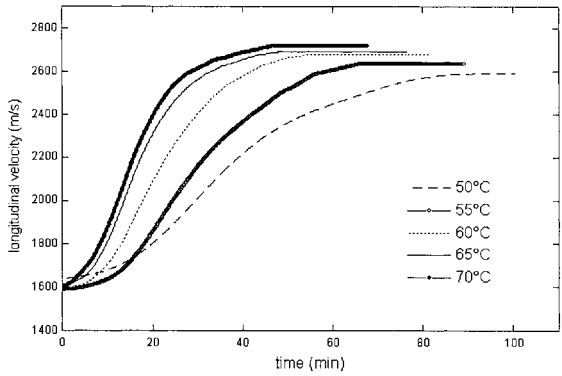

Figure 5. Longitudinal velocity measured at different cure temperatures.

The attenuation (Δ) is calculated measuring the amplitude of the ultrasonic waves in presence and absence of the sample and monitoring the thickness changes (d) during cure, according with:

$$\Delta = -\frac{1}{d(t)} \ln\left(\frac{A_{II}}{A_I}\frac{1}{T_{21}T_{12}}\right) \tag{6}$$

where A_I and A_{II} are the amplitudes measured without and with the sample between the transducers and T_{21} and T_{12} the transmission coefficients at the interfaces resin-transducer and transducer-resin respectively calculated from the acoustic impedances of the delay line of the transducer and of the resin[4].

The attenuation calculated using Eq.6 is reported in Fig.6. After a peak, corresponding to the vitrification as is detected at so high frequencies[3,4], the reduction of mechanical coupling between transducer and resin lead to a limited reduction of the attenuation detected in pulse echo measurements[4]. For this reason correct attenuation values are measured up to a small time interval after the peak.

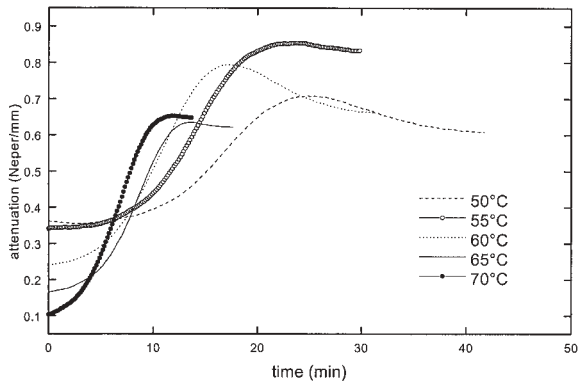

Figure 6. Ultrasonic attenuation measured at different cure temperatures.

When the sample dimension normal to the acoustic wave is large compared with respect to the wavelength, the wave propagation is governed by the complex bulk longitudinal modulus L* = L'+ iL". This complex modulus is related to the bulk (K*) and shear (G*) complex moduli[10] L*=K*+4/3G*. L' corresponds to the stiffness of a system that is deformed changing its dimensions in one direction while in the other two directions the dimensions are constrained to be constant, as it occurs in samples where two dimensions are much larger than the third. For a liquid or a soft rubbery material K'>>G' and L' may be considered equal to the bulk modulus, while K" and G" may be of the same order of magnitude and the effect of G" on L" cannot be neglected.

The measurements of ultrasonic longitudinal velocity (V_L) and attenuation (Δ) may be used for the calculation of the storage (L') and loss (L") bulk longitudinal moduli[9]:

$$L' = \frac{\rho V_L^2\left[1-\left(\frac{\Delta\lambda}{2\pi}\right)^2\right]}{\left[1+\left(\frac{\Delta\lambda}{2\pi}\right)^2\right]^2} \qquad L'' = \frac{2\rho V_L^2\left(\frac{\Delta\lambda}{2\pi}\right)}{\left[1+\left(\frac{\Delta\lambda}{2\pi}\right)^2\right]^2} \tag{7}$$

where ρ is the material density and λ is the wavelength, given by $\lambda = V_L/\nu$ as a function of the frequency, ν. For the studied case the effect of attenuation on the values of L' was negligible and a single longitudinal modulus $L = \rho V_L^2$ can be calculated. The difference between L and L', up to the attenuation peak, was lower than 3% and hence only L has been calculated.

A comparison between the degree of reaction calculated by DSC and L is reported in Fig.7 for one of the isothermal tests. At the beginning of the cure the degree of reaction obtained by DSC grows more rapidly than the longitudinal velocity as a consequence of the high concentration of reactive groups in the liquid reactive mixture. On the other hand, the growth of molecular weight in form of branched oligomers, has a limited effect on the mechanical properties of the resin before the gel point. Close to gelation, the growing branched molecules are characterized by extensive entanglements capable to provide an elastic response measured as a significant growth of longitudinal velocity and L. In the last part of the cure, a moderate or negligible increase of the degree of reaction is accompanied by a significant increase of L.

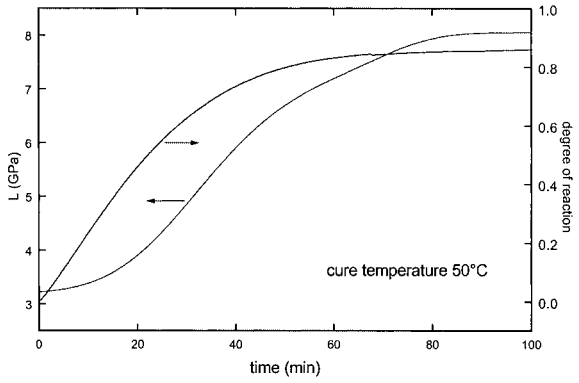

Figure 7. Comparison of time dependence of longitudinal modulus and degree of reaction.

Taking the values of L and α at corresponding times, the plot of L as a function the degree of reaction shown in Fig.8 is obtained for three cure temperatures. These data indicate that L is mainly sensitive to the increasing crosslinking density occurring after gelation rather than to the number of reacted groups. Therefore a strong non linear correlation between L and α is observed.

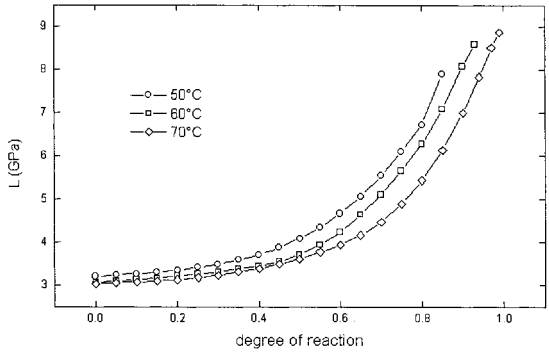

Figure 8. Longitudinal modulus as a function of the degree of reaction obtained combining DSC and ultrasonic data plotted in the former figure.

Nevertheless, the evolution of mechanical properties after gelation is theoretically predicted by Flory [9] in the theory of rubber elasticity and may be computed, for example, applying the statistical approach of Macosko and Miller[5,6]. Then L could be better correlated with the degree of crosslinking, defined as the concentration of effective junction points in the infinite network, rather than with the degree of reaction. The theory of Miller and Macosko for stepwise polymerization leads to the calculation of the crosslinking density (μ) and the concentration of active network chains (ν) through the determination of $P(F_A^{out})$, the probability that the event F_A^{out} occurs. For the studied system F_A^{out} is defined as the event that taking any amine group and moving out from the molecule to which the group is connected a dangling chain is reached. The theory derives an expression which provides $P(F_A^{out})$ as a function of the amine conversion p_A that, as mentioned above, can be assumed equal to α_{DSC}. Then for the studied formulation, characterized by r=0.556, the following equation is obtained:

$$rp_A^2 P(F_A^{out})^5 - P(F_A^{out}) - rp_A^2 + 1 = 0 \tag{8}$$

$P(F_A^{out})$ is calculated for different values of p_A using a numerical solution of Eq.8. Afterwards, an expression of $P(F_A^{out})$ as a fuction of the degree of conversion of amine groups is obtained by polinomial fitting. In particular for the postgel range of p_A (p_A>0.6) a simple third order polinomial expression is obtained:

$$P(F_A^{out}) = a_0 + a_1 p_A + a_2 p_A^2 + a_3 p_A^3 \tag{9}$$

where: α_0= 2.675, α_1= - 4.337, α_2= 3.262, α_3= -1.145.

A plot of $P(F_A^{out})$ vs conversion of amine groups as obtained from Eq.9 is shown in Fig.9. This expression is valid in postgel region only, where the infinite network is developed. For $\alpha<\alpha_{gel}$, in presence of molecules of finite size, $P(F_A^{out})$ is assumed equal to unity, as Eq.8 has no physical meaning.

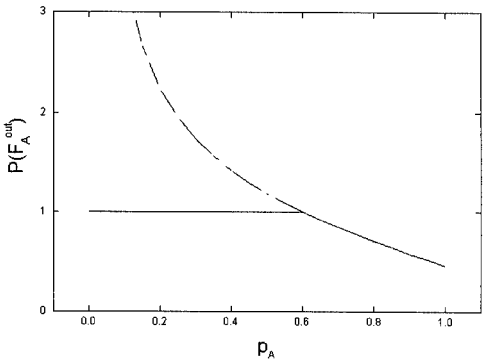

Figure 9. Plot of $P(F_A^{out})$ vs conversion of amine groups as obtained from Eq.9.

Once $P(F_A^{out})$ is calculated, the probability that an amine molecule is connected to m segments, belonging to the infinite network, is:

$$P(X_{m,6}) = \binom{6}{m} P(F_A^{out})^{6-m} \left[1 - P(F_A^{out})\right]^m \tag{10}$$

An amine molecule is an effective crosslinking point only if m>3. The value of $P(X_{m,6})$ are reported in Fig.10 for m ranging between 3 and 6; these values of m corresponds to the development of an effective crosslink. As a consequence of the large excess of epoxy, the probability of finding 6 reacted hydrogen of the amine monomer is very low and limited to the last part of the reaction.

Then the crosslinking density, μ, is given by:

$$\mu = [A_0] \sum_{m=3}^{6} P(X_{m,6}) \tag{11}$$

where $[A_0]$ represents the initial concentration of amine equal to: $5.52*10^{-4}$ moli/cm^3. The sum is between m=3 and m=6 being these values capable to generate a junction between 3 to 6 chains segments. Observing that at each junction point can be associated m/2 connected chain segments the concentration of the active network chains, ν, is

obtained as :

$$\nu = [A_0] \sum_{m=3}^{6} \frac{m}{2} P(X_{m,6}) \tag{12}$$

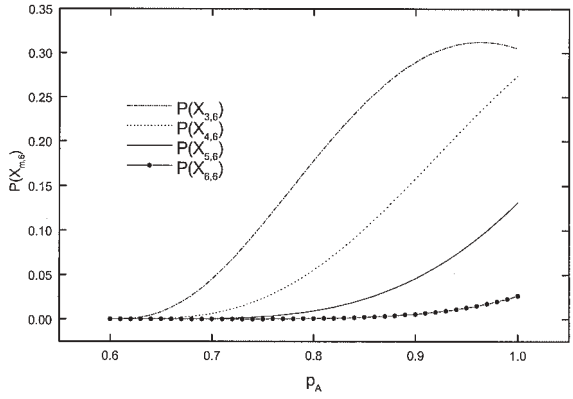

Figure 10. Probability, $P(X_{m,6})$, that an amine molecule, belonging to the infinite network, is connected to m segments, as a function of the amine groups conversion, p_A.

Fig.11 shows a plot of μ and ν as a function of p_A, as obtained by eqs. 11 and 12.

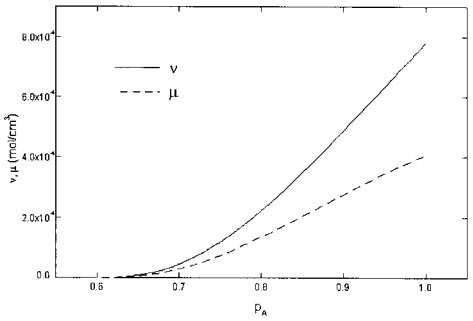

Figure 11. Crosslinking density, μ, and concentration of the active network chains, ν, as a function of the amine groups conversion.

Combining Eqs. 8 through 12 the dependence of L on ν is obtained. As shown in Fig.12 a large part of the curves at every temperature is linear as predicted by the theory of rubber elasticity for the shear modulus. If a linear dependence on ν is assumed for shear, G, and Young, E, moduli then also the bulk modulus K and hence L should be characterized by the same dependence, since:

$$K = \frac{\frac{E}{3}}{3 - \frac{E}{G}} \tag{13}$$

However, as reported by Nielsen[11], the theory of rubber elasticity predicts moduli far too small for extremely high crosslinked materials. Despite of these limitations, in this case a linear correlation between L and the concentration of active network chain is observed during crosslinking as also observed by Nielsen[11].

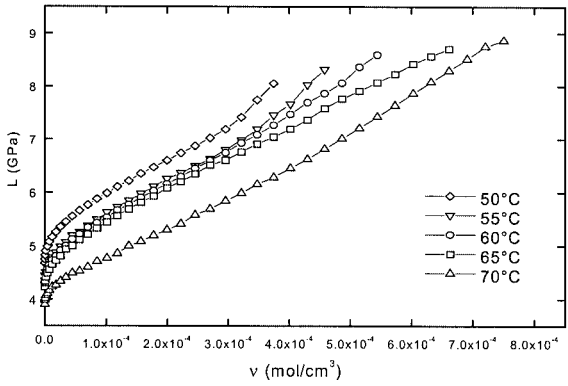

Figure 12. Correlation between L and the concentration of active network chains, ν, after the gel point.

The deviation from linearity close to the gel point in Fig.12 can be the consequence of errors arising both, from ~~of~~ the choice of a theroretical value for α_{gel} and from the assumption of $p_A=\alpha_{DSC}$. A further deviation from linearity is observed at the end of the reaction for isothermal cure at 50, 55 and 60 °C. DSC analysis (Table 1) indicates that at these temperatures α_{max} and T_g are quite lower than 1 and T_{gmax}=91 °C respectively. This indicates that vitrification occurs during reaction leading to a diffusion controlled reaction termination. Therefore the non linearity in the last part of the L vs. ν curves at these three temperatures can be associated to this transition to a glassy state. This transition could be responsible of a faster increase of L with ν.

However, as shown in Fig.12, the linear growth of the modulus with temperature, predicted by the theory of rubber elasticity, is not observed. This may be explained considering that the very small deformation applied by ultrasonic wave propagation involves only energetic intrachain interactions rather than entropic effects associated

with macroscopic stretching of the chain segments[12]. In fact the energetic contribution to the elastic response of a rubber, not dependent on the strain, may be dominant at very small strains[12]. This result, in contrast with the observed linear dependence of L on v, suggests that the entropic contribution to the ultrasonic bulk longitudinal modulus is not relevant. In this case the results of Fig.11 could be explained simply considering that the crosslinking is associated with a significant stiffening of the materials thanks to the introduction of strong constraints to the molecular mobility. α measures each reaction steps either leading to a simple chain extension or to additional crosslinking during the network growth. On the other hand v, representative only of the development of crosslinking segments, appears to significantly affect the stiffness of the resin. An additional stiffening effects is observed as an increase of L in Fig.11, in correspondence of the vitrification. Therefore the presented results indicates that the ultrasonic longitudinal modulus of the rubbery epoxy shows a linear dependence on this event.

Conclusions

The isothermal crosslinking of a model epoxy resin cured with an exa-functional amine is studied using propagation of longitudinal ultrasonic wave. The ultrasonic velocity and attenuation, measured by a transmission technique, have been applied to the calculation of the bulk longitudinal modulus. The comparison of ultrasonic and DSC data have indicated that the most significant change of the ultrasonic modulus starts close to gelation. Therefore, a correlation between the ultrasonic modulus and the crosslinking density is proposed using the statistical theory of Miller and Macosko. Then, the degree of reaction obtained by DSC and the concentration of active network chains are correlated on the base of the stoichiometry of epoxy and amine monomers. The longitudinal modulus plotted as a function of the concentration of active network chains showed a linear dependence in the rubbery region, while in the last part of the reaction, the transition to the glassy state is reflected in a sudden growth of the storage modulus. However, the longitudinal modulus, for each value of the crosslinking density, decreases with temperature, in contrast with theory of rubber elasticity. This result suggested that the entropic contribution to the ultrasonic bulk longitudinal modulus is not relevant as a consequence of the small deformation involved in the propagation of the ultrasonic waves.

References

[1] D. Lairez, D. Durand, J.R. Emeryl, *Makromol. Chem, Macromol. Symp.* 45 (1991) p. 31
[2] I. Alig, D. Lellinger, K. Nancke, A. Rizos and G. Fytas *J. Appl. Polym. Sci.* 44 (1992) p. 829
[3] M. Matsukawa and I. Nagai, *J. Acoust. Soc. Am.* 99 (1996) p. 2110
[4] A. Maffezzoli, E. Quarta, V.A.M. Luprano, G. Montagna, L. Nicolais *J. Appl. Polym. Sci.,* 73 (1999) p. 1969
[5] C.V. Macosko, D.R. Miller, *Macromolecules*, 9, (1976), p. 199
[6] D.R. Miller, C.W. Macosko, *Macromolecules*, 9, (1976), p. 206
[7] K. Dusek, *Network formation in Curing of Epoxy Resins,* Dusek, 1985
[8] G. Odian, *Principles of polymerization*, McGraw-Hill, New York, 3rd edn, 1991
[9] P.J.Flory *Priciples of polymer chemistry* Cornell University Press, Ithaca N.Y. 1953
[10] J.D. Ferry, *Viscoelastic Properties of Polymers*, John Wiley and Sons, New York, 1980
[11] L.E. Nielsen and R.F. Landel, Mechanical properties of polymers and composites Marcel Dekker N.Y USA (1994)
[12] J.J. Aklonis and W.J. MacKnight *Introduction to polymer viscoelesticity* Wiley Interscience N.Y. (1982)